Optimal synthesis of rotating packed bed reactor

Zhi Qian[1], Ignacio E. Grossmann*[2]

1 University of Chinese Academy of Sciences, Beijing 100049, People's Republic of China.

2 Department of Chemical Engineering, Carnegie Mellon University, Pittsburgh, Pennsylvania 15213, United States

* Corresponding author. Tel.: +1 412 268 2230; fax: +1 412 268 7139.

E-mail address: grossmann@cmu.edu (I.E. Grossmann).

ABSTRACT

Rotating packed bed (RPB), a novel apparatus involving process intensification (PI), has been successfully used in the chemical industry in recent decades. In this paper, we establish a connection between process integration and process intensification for which we propose a superstructure involving a RPB and a packed bed (PB) in order to determine the optimal integrated design. We describe models to predict flow performance and design of RPB and PB. These are used as a basis to set up the optimization models for RPB and PB which are incorporated in a superstructure that considers configurations in series, in parallel and in between. The optimization of the superstructure is formulated as a nonlinear programming problem. The application of the proposed synthesis model is demonstrated with a case study with H_2S removal from plant tail gas.

1. Introduction

Process intensification has been defined by Ramshaw in 1995[1] as a methodology for making remarkable reduction in equipment size, energy consumption or waste production to reach a given production goal. Process intensification is motivated by the desire for a breakthrough on a novel apparatus resulting in cost effective, sustainable technology. Process intensification [2-4] has become an increasingly popular topic. Process synthesis[5] as an assembly and interconnection of units for efficient performance and low energy consumption process should be well suited for process intensification[6]. Therefore, an intensification process based on superstructure optimization could lead to a novel way to integrate both conventional and intensified process units.

Rotating packed bed is a typical PI operation unit [6-8], which is compact, of low investment and high efficiency, and widely used in gas purification, distillation and nano-material preparation[9-14]. Fig. 1 shows the comparison between RPB and traditional PB for an industrial desulfurization process[15]. Compared to the tower, the volume mass transfer coefficient within RPB increases 1−2 orders of magnitude, with which the volume of RPB is only 9% of the PB.

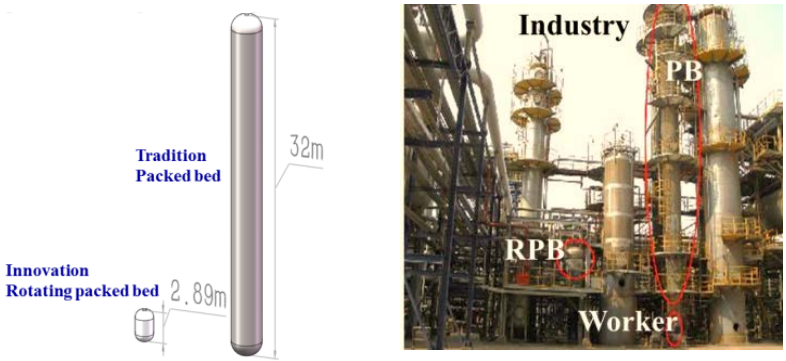

Fig. 1 The comparison between RPB and PB within an industry case

However, RPB is a rotating equipment and requires significant energy input. As shown with an example in Table 1, RPB has a distinct advantage over PB on the investment and space it occupies. However, the RPB compared to the PB requires a motor to provide rotation. Therefore, there is a tradeoff between RPB and PB. Process

intensification and integration can be coupled to search for novel processes that combine both technologies as shown in Fig. 2.

Table 1 Rotating packed bed vs packed bed[15]

	Rotating Packed Bed	Packed Bed
Height	2.89 m	32 m
Equipment volume	3.4 m^3	36 m^3
Motor	37kW	--
H_2S content in exit gas	< 20ppm	< 20ppm

In this paper, nonlinear programming models are first presented to optimize separately the RPB and the PB. Next a superstructure optimization model is proposed to synthesize configurations that integrate the advantages of packed bed, which is a static equipment with no energy input, and rotating packed bed, which has high mass transfer efficiency.

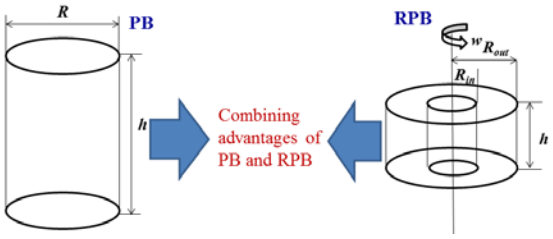

Fig. 2 Processes in-between combining process intensification and integration

In order to synthesize a design involving RPB and PB units the superstructure shown in Fig. 3(a) is proposed, in which the liquid and gas streams are distributed among potential streams for their countercurrent flow. RPB and PB are interconnected with potential streams to integrate both advantages to accomplish not only decreasing the volume of the units, but to reduce the energy consumption. The configuration between RPB and PB could be in series shown in Fig. 3(b) or in parallel shown in Fig. 3(c), and even something in-between which will be decided by parameters provided and optimization results. The goal is to minimize the total cost of the integrated system. The synthesis problem is formulated as a nonlinear programming (NLP) model that involves constraints corresponding to the performance of the RPB and PB, the intensification mechanism of mass transfer, end-effect quantification of RPB, and

mass balance in the process.

2. Problem statement

2.1 Problem description.

In this work both Rotating Packed Bed (RPB) and Packed Bed (PB) are interconnected using mixer unites (MU) and splitter units (SU) to develop the superstructure shown in Fig.3a. Gas streams (solid line) and liquid streams (dash line) are supplied to the two treatment units. After these gas streams are contacted countercurrently with liquid steams in the units, both gas and liquid are recycled to the treatment units or sent to the outlet stream that must satisfy maximum limit on the concentration of the sweet gas.

The sizes and design parameters of RPB and PB are variables to be determined by each gas purifying specification and treatment capacity. The flowrates and concentration of the gas and the liquid in each stream are also variables to be determined. Using mass transfer models for the RPB and the PB, fairly accurate design and operating conditions can be obtained. The objective is to select the optimal configuration involving the RPB and the PB so as to minimize the total investment and operating costs.

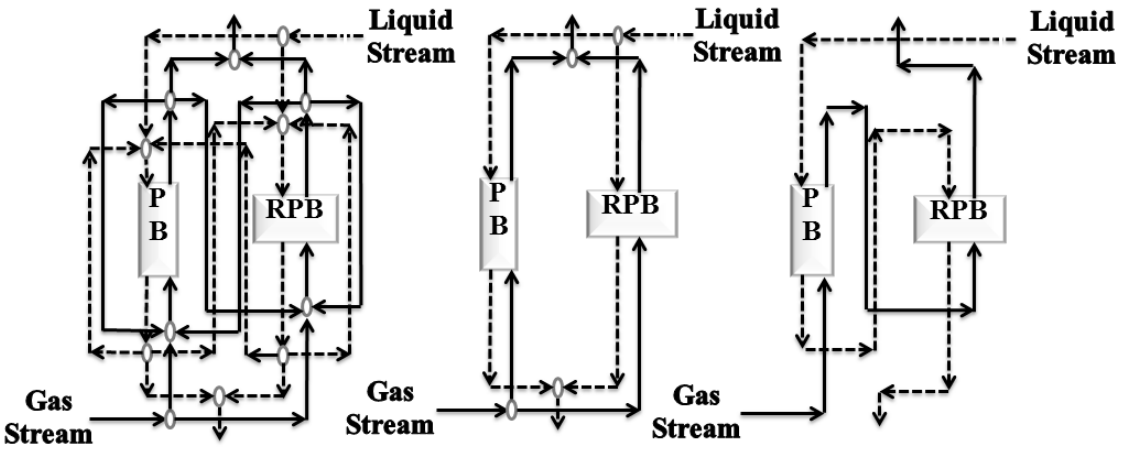

(a) (b) (c)

Fig. 3 Superstructure of the integrated RPB and PB processes: (a) overall structure; (b) in parallel configuration; (c) in series configuration

2.2 Mathematical programing models

The mathematical models of integrated RPB and PB processes are based on models presented in section 3, which consist of mass transfer process intensification mechanisms, fluid flow expressions and mass balance equations. The optimization models are formulated as nonlinear programing (NLP) problems. Some of the assumptions involved in the modeling are the following:

(1) The total gas treatment capacity and inlet/outlet gas concentration are fixed.

(2) Only gas with single dissolvable species is considered.

(3) The flow pattern in the RPB and PB are plug flow.

(4) Both the RPB and the PB operate isothermally.

(5) Both correlations between the investment cost and the equipment volume and between electricity cost for liquid pump and liquid flowrate are linear.

3. The description of process intensification

The superstructure in Fig. 3(a) connects process intensification and integration together, and makes it feasible to seek novel processes comprised of RPB and PB. However, the crucial issue is that the intensification mechanism of mass transfer and end-effect must be modeled as part of the superstructure optimization. The purpose of this section is to describe the intensification process mentioned previously and consider it as an important design consideration. Based on the micro-mechanisms of intensification, we generally categorize the mechanisms as two types. The first one is kinetics based and the second one is flow based.

3.1 Kinetics based intensification mechanism of mass transfer

As for the gas-liquid mass transfer process within a RPB, the intensification of RPB is mostly obtained by the continuous renewal of liquid film in the rotating packing. A sharp concentration profile of the dissolvable gas in liquid film, as shown in Fig. 4, will be formed when the liquid enters the rotating packing, which the shorter lifetime of liquid film is, the higher mass transfer coefficient is.

Based on mass transfer coupling with reaction, a partial differential equation model with chemical absorption of species *i*, which for instance can be CO_2 or H_2S, is set up to describe the mass transfer process in the liquid film within a RPB[16].

$$\begin{aligned} &\frac{\partial c_i}{\partial t} = D_i \frac{\partial^2 c_i}{\partial x^2} - k_{i,ov}(c_i - c_{i,eq}) \\ &c_i(x,0) = c_{i,eq} \\ &c_i(0,t) = c_{i,0}, c_i(\infty,t) \le c_{i,eq}, 0 < x < \infty, t > 0 \end{aligned} \tag{1}$$

Then the concentration of dissolvable gas in liquid film can be obtained by solving the above partial differential equation [16]:

$$\begin{aligned} c_i = &\frac{c_i - c_{i,eq}}{2} \exp(-x\sqrt{\frac{k_{i,ov}}{D_i}}) erfc(\frac{x}{2\sqrt{D_i t}} - \sqrt{k_{i,ov} t}) + \\ &\frac{c_i - c_{i,eq}}{2} \exp(x\sqrt{\frac{k_{i,ov}}{D_i}}) erfc(\frac{x}{2\sqrt{D_i t}} + \sqrt{k_{i,ov} t}) + c_{i,eq} \end{aligned} \tag{2}$$

According to first Fick's law the liquid-side mass transfer coefficient (k_L) can be calculated from the following equation[16].

$$k_L = \frac{\sqrt{k_{i,ov} D_i}}{\bar{t}} \left[\bar{t} erf(\sqrt{k_{i,ov} \bar{t}}) + \sqrt{\frac{\bar{t}}{\pi k_{i,ov}}} \exp(-k_{i,ov} \bar{t}) + \frac{1}{2k_{i,ov}} erf(\sqrt{k_{i,ov} \bar{t}}) \right] \tag{3}$$

Here $\bar{t}$ is the average lifetime of the liquid film which is renewed every time as it passes through one layer of packing of RPB. The $\bar{t}$ is decided by both the liquid residence time and the number of packing layers.

The comparison between Rotating Packed Bed and Packed Bed with mass transfer coefficient can be seen in Fig. 4, which illustrates that the mass transfer coefficient surges as the mean lifetime of liquid film descends. Take the MDEA (Methyldiethanolamine)-CO_2 reactive absorption with a temperature of 293K and fluid flow rate of 6L/h for instance, when the mean lifetime of liquid film is shorter than 2s as the rotating speed of the RPB increases, a strong intensification effect will appear. As the plot shows, the intensification increases rapidly with a decline of the

lifetime of liquid film and makes the dynamic-state mass transfer much higher than the static-state one. If the mean lifetime of the liquid film is approximately to zero, the intensification will become infinity which means that there is no liquid-phase resistance.

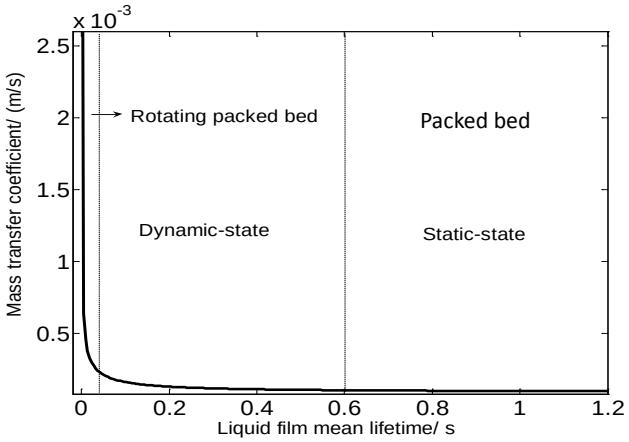

Fig. 4 Comparison between RPB and PB on mass transfer coefficient[16]

The mean lifetime of liquid film in a static device, such as packed bed, is longer than 2s and in this case the mass transfer coefficient gradually levels off and the dynamic-state mass transfer changes into the static state. Take the example of the absorption of CO_2 by 10% MDEA at temperature of 293K and fluid flow rate of 6L/h, given t of 2s, the ratio $(k_{L,dynamic})/(k_{L,static})$ is about 1.02.

3.2 Flow based process intensification within RPB

The end-effect zone of packing, which is the area that ranges from the inner edge of the packing to the point liquid being captured by the rotating packing, is the most significant section for mass transfer within RPB because of the maximum relative velocity between liquid and rotating packing. In this region, the liquid is intensely torn and sheared and the liquid film is renewed with high frequency. Then the mass transfer process is sharply intensified. A modeling study on the end-effect zone plays an important role in quantifying the process intensification and optimizing the design to make the RPB as small as possible.

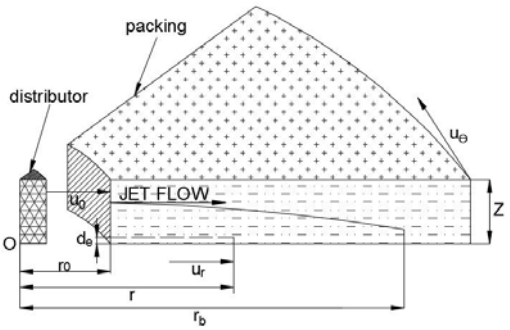

Fig. 5 The diagram of jet penetration depth within rotating packing[17]

We propose a hypothesis of liquid-capture mechanism to describe the end-effect zone of RPB[17]. As shown in Fig.5, the jet flow will be gradually captured by the rotating packing in circumferential direction after the liquid is sprayed into the packing by distributor, which means all the liquid will be transferred from the initial radial direction to the ultimate circumferential direction in the end-effect area. To establish the cylindrical coordinate system, the rotor axial direction is set as *z* axial, the radial direction is set as *r*, and the tangential direction is set as θ. The equation is given by the Navier−Stokes (N-S) equation[17]:

$$\begin{aligned} &\frac{\partial u_\theta}{\partial t} = \nu_L \frac{\partial^2 u_\theta}{\partial z^2} \\ &t = 0, u_\theta = 0 \\ &z = 0, u_\theta = rw, t > 0 \\ &z = \infty, u_\theta = 0, t > 0 \end{aligned} \tag{4}$$

This model is the momentum balance equation that describes the velocity distribution in the liquid film under the influence of viscous force. Based on the simplified N-S model and mass balance equation to get the length of end effect zone can be obtained as shown below. Please refer to reference [17] for details of this model.

$$L = r_b - r_0 = \sqrt{\frac{d_e u_0}{0.265w} + r_0^2} - r_0 \tag{5}$$

where $d_e = \frac{4\varepsilon}{\alpha}$, d_s is the equivalent diameter of virtual tube in the packing in

meters[18].

Equation (5) predicts the length that ranges from the inner edge of the packing to the point the liquid is being captured by rotating packing. Using equation (5) we can at least define half of the packing of RPB as end-effect zone to optimize the design of RPB. Then the nonlinear programming model can be developed based on the understanding of kinetics and flow properties.

4. Optimization models integrated with process intensification

In this section the optimization models based on process intensification mechanisms are presented. Nonlinear programing models are developed for RPB and PB, respectively. Next a nonlinear programming model is proposed to optimize the superstructure in Fig. 3a to obtain the optimal configuration and design parameters of the synthesized structure.

4.1 Nonlinear programing model for RPB only

The objective function of the NLP (P1) is to minimize the total cost C_{RPB} of single RPB system, which has the annual electricity cost for rotor, the annual electricity cost for liquid pump and the annualized investment cost for the equipment. The first term of the objective function describes the rotational power of RPB and it is linear with the electricity consumption. The second term is the electricity consumption of the liquid pumping, and the last one is the annualized cost of the RPB relating to its own volume.

Mass transfer process intensification equation, mass balance, liquid velocity, average lifetime of liquid film and end-effect length equation are the constraints of the NLP model (P1) below. The objective is to select the inner radius, outer radius, axial height and rotating speed of RPB packing shown in Fig. 6 in order to minimize the annualized investment and operating cost. The last inequality shows at least half of packing is end-effect area for the optimal design of RPB.

$$\min C_{RPB} = c_{RPB,1}\rho L_{RPB} w^2 (R_{out}^2 - R_{in}^2) + c_{RPB,3} L_{RPB} + c_{RPB,2}\pi h_{RPB} (R_{out}^2 - R_{in}^2) \quad \text{(P1)}$$

s.t.

$$k_L = \frac{\sqrt{k_{ov} D}}{\bar{t}} \left[\bar{t} erf(\sqrt{k_{ov} \bar{t}}) + \sqrt{\frac{\bar{t}}{\pi k_{ov}}} \exp(-k_{ov} \bar{t}) + \frac{1}{2k_{ov}} erf(\sqrt{k_{ov} \bar{t}}) \right]$$

$$G \ln\left[\frac{y_{in}}{y_{out}(1 - y_{in})} - 1 \right] = k_L \alpha h_{RPB} \pi (R_{out}^2 - R_{in}^2)$$

$$u = 0.02107 L^{0.2279} (wR)^{0.5488}$$

$$R = R_{out} - R_{in} \qquad \bar{t} = \frac{R}{u N_s}$$

$$0 \le R_{out} - R_{in} \le 2\left[\sqrt{\frac{d_e u}{0.265 w} + R_{in}^2} - R_{in} \right]$$

$$0.5 R_{out} - R_{in} \ge 0 \qquad 3R_{in} - R_{out} \ge 0$$

$$L, w, h, \bar{t}, u, d_e, R_{out}, R_{in} \ge 0$$

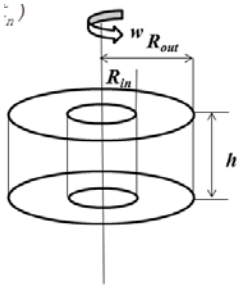

Fig.6 The diagram of the packing of RPB with design parameters

It should be noted that the NLP (P1) is nonconvex and therefore it may potentially give rise to multiple local optima.

4.2 Nonlinear programing model for PB only

The objective function of NLP (P2) is to minimize the total cost of single PB system, which involves the annual electricity cost for liquid pump and the annualized investment cost for the equipment relating to its own volume.

The constraints involve the mass transfer coefficient equation, mass balances and average lifetime of liquid film. The objective function is to select the optimal radius and height of PB as shown in Fig.7. The lifetime of liquid film in PB is usually longer than 2 seconds and it is enough time for dissolvable gas to form a stable concentration gradient in liquid film, which means the mass transfer in PB is steady and process

intensification does not apply. Therefore, we set $\bar{t} = 2$.

$$\min C_{PB} = c_{PB,1}\pi h_{PB} R_{PB}^2 + c_{PB,2} L_{PB} \qquad \text{(P2)}$$

s.t.

$$k_L = \frac{\sqrt{k_{ov} D}}{\bar{t}} \left[\bar{t} erf(\sqrt{k_{ov} \bar{t}}) + \sqrt{\frac{\bar{t}}{\pi k_{ov}}} \exp(-k_{ov} \bar{t}) + \frac{1}{2k_{ov}} erf(\sqrt{k_{ov} \bar{t}}) \right]$$

$$G \ln\left[\frac{y_{in}}{y_{out}(1 - y_{in})} - 1 \right] = k_L \alpha h_{PB} \pi R_{PB}^2$$

$$\bar{t} = 2 \qquad h_{PB}, R_{PB}, L_{PB}, \bar{t} \geq 0$$

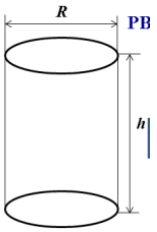

Fig.7 The diagram of the PB with design parameters

It should also be noted that the NLP(P2) is nonconvex and therefore it may potentially give rise to multiple local optima.

4.3 Nonlinear programing for superstructure optimization

We consider the superstructure of Fig. 3a in order to determine the optimal configuration of a system involving either the RPB or the PB, or a combination of both in series or in parallel.

We consider the models in section 4.1 and 4.2 in order to set up the NLP model (P3) of the superstructure in Fig. 3a. The objective function of NLP (P3) involves the annual electricity cost for the rotor, the annual electricity costs for the liquid pumps and the annualized investment costs for the equipment. Mass balances for gas streams and liquid streams are included as well as corresponding mass transfer process and liquid flow equations.

Objective function:

$$\min C_S = c_{RPB,1}\rho L_{RPB} w^2 (R_{out}^2 - R_{in}^2) + c_{RPB,2}\pi h_{RPB}(R_{out}^2 - R_{in}^2) + c_{RPB,3} L_{RPB} c_{PB,1} \pi h_{PB} R_{PB}^2 + c_{PB,2} L_{PB} \quad \text{(P3)}$$

Mass balance equations

Gas phase

$$G_{S1} = G_{S2} + G_{S3}$$

$$G_{S3} y_{3,PB} + G_{S8} y_{8,PB} + G_{S12} y_{12,PB} = G_{S4} y_{4,PB}$$

$$y_{out,PB} = \frac{y_{in,PB}}{\left[\exp\left(\frac{k_{L,PB}\alpha h_{PB}\pi R_{PB}^2}{G_{s4}}\right) + 1\right](1 - y_{in,PB})}$$

$$G_{S4} = G_{S5} + G_{S12}(y_{in,PB} - y_{out,PB})$$

$$G_{S5} = G_{S8} + G_{S7} + G_{S6}$$

$$G_{S2} y_{2,RPB} + G_{S7} y_{7,RPB} + G_{S13} y_{13,RPB} = G_{S9} y_{9,RPB}$$

$$y_{out,RPB} = \frac{y_{in,RPB}}{\left\{\exp\left[\frac{k_{L,RPB}\alpha h_{RPB}\pi (R_{out}^2 - R_{in}^2)}{G_{s4}}\right] + 1\right\}(1 - y_{in,RPB})}$$

$$G_{S9} = G_{S10} + G_{S9}(y_{in,RPB} - y_{out,RPB})$$

$$G_{S10} = G_{S12} + G_{S13} + G_{S11}$$

$$G_{S14} = G_{S6} + G_{S11}$$

Liquid phase

$$L_{S1} = L_{S2} + L_{S3}$$

$$L_{S3} + L_{S8} + L_{S12} = L_{S4}$$

$$L_{S4} = L_{S5}$$

$$L_{S5} = L_{S8} + L_{S7} + L_{S6}$$

$$L_{S2} + L_{S7} + L_{S13} = L_{S9}$$

$$L_{S9} = L_{S10}$$

$$L_{S10} = L_{S12} + L_{S13} + L_{S11}$$

Constraints

$$k_{L,RPB} = \frac{\sqrt{k_{ov} D}}{\bar{t}}\left[\bar{t}\,\mathrm{erf}(\sqrt{k_{ov}\bar{t}}) + \sqrt{\frac{\bar{t}}{\pi k_{ov}}}\exp(-k_{ov}\bar{t}) + \frac{1}{2k_{ov}}\mathrm{erf}(\sqrt{k_{ov}\bar{t}})\right]$$

$$k_{L,PB} = \frac{\sqrt{k_{ov} D}}{u^{0.2102} L^{0.2279} (wR)^{0.5488}}\left[2\mathrm{erf}(\sqrt{2k_{ov}}) + \sqrt{\frac{2}{\pi k_{ov}}}\exp(-2k_{ov}) + \frac{1}{2k_{ov}}\mathrm{erf}(\sqrt{2k_{ov}})\right]$$

$$R = R_{out} - R_{in} \qquad \bar{t} = \frac{R}{uN_S}$$

$$0 \le R_{out} - R_{in} \le 2\left[\sqrt{\frac{d_e u}{0.265w} + R_{in}^2} - R_{in}\right]$$

$$0.5R_{out} - R_{in} \ge 0 \qquad 3R_{in} - R_{out} \ge 0$$

$$G_{S4} \ln\left[\frac{y_{in,PB}}{y_{out,PB}(1 - y_{in,PB})} - 1\right] = k_{L,PB}\alpha h_{PB}\pi R^2$$

$$G_{s9} \ln\left[\frac{y_{in,RPB}}{y_{out,RPB}(1 - y_{in,RPB})} - 1\right] = k_{L,RPB}\alpha h_{RPB}\pi(R_{out}^2 - R_{in}^2)$$

$$L, w, h_{RPB}, \bar{t}, u, d_e, R_{out}, R_{in}, h_{PB}, R_{PB}, L_{PB} \ge 0$$

Note that the NLP (P3) is also nonconvex and includes bilinear terms for the mass balances which could make the model prone to having multiple local optima.

5. H_2S purification case study

In order to apply the NLP models in the previous section, we consider a case study on a desulfurization process for crack gas at a refinery in China which is shown in Fig.1. The gas contains about 1vol% H_2S. The large amount of H_2S is not only a hazard to human health and contaminates the environment, but its high corrosiveness leads to a high cost for pipeline repair and replacement. For the wire mesh packing, the porosity, ε, is 0.97, and the total specific surface area, *a*, is 220 m^2/m^3. The jet initial velocity is 6m/s before it enters into the rotating bed. The other physical parameters for the H_2S purification case study are presented in Table2. We solve the NLP models for RPB (P1), for PB (P2) and superstructure (P3) using GAMS IPOPT 3.12 and CONOPT 3. The results are presented in Tables 3 and 4.

Table 2 Parameters for H_2S purification case study

	Rotating Packed Bed	Packed Bed
Content of H_2S	10,000 (ppm)	10,000 (ppm)
Gas flow	10,000 (m^3/hr)	10,000 (m^3/hr)
Liquid film renewal times	90	--
Operating cost scale factor for Rotation, $c_{RPB,1}$	2.2 (10,000 CNY/kw)	--
Operating cost factor for RPB volume, $c_{RPB,2}$	121 (10,000 CNY/m^3)	--
Investment scale factor for PB volume, $c_{PB,1}$	--	5 (10,000 CNY/m^3)
Operating cost scale factor for RPB liquid pumping, $c_{RPB,3}$	1 (10,000 CNY·hr/m^3)	--
Operating cost scale factor for PB liquid pumping, $c_{PB,2}$	--	1.6 (10,000 CNY·hr/m^3)
Diffusion coefficient, D	1.2×10^{-9} (m^2/s)	1.2×10^{-9} (m^2/s)
Reaction rate constant of H_2S with amine, k_{ov}	1.5×10^{8} (1/s)	1.5×10^{8} (1/s)
H_2S content in exit gas	<100 (ppm)	< 100 (ppm)

Table 3. Comparison between separate reactors and solution from superstructure.

	RPB (Rotating packed bed)	PB (Packed bed)	RPB-PB	
			RPB	PB
Height/*m*	0.347	15.275	0.273	7.449
Radius/*m*	0.575 (Out)	0.544	0.452(Out)	0.477
	0.192 (In)		0.151(In)	
Volume/m^3	0.321	14.2	0.156	5.312
Rotating speed/*r/min*	600	--	660	--
Capacity for gas /m^3/*hr*	10008	10008	4845.6	5162.4
Liquid /m^3/*hr*	50	100	25.2	50.4
Equivalent annual cost for equipment /10,000 RMB	38.799	71.002	18.872	26.562

Annual electricity cost for rotor /10,000 RMB	25.915	--	6.318	--
Annual electricity cost for liquid pump /10,000 CNY	5.112	15.926	2.427	8.271
Structure	Individual	Individual	In parallel (b in Fig.3)	
Gross cost /10,000 CNY	69.826	86.928	62.449	

Table 3 shows the comparison of the design parameters between the separate reactors and the solution of the superstructure that are obtained from the corresponding NLP models. Under a certain gas treatment capacity, the single PB requires the highest total annual cost and the single RPB takes the second place. The optimal alternative is a hybrid combination of RPB and PB in parallel (see Fig 3b), which requires the lowest annual cost, yielding savings of 11.2% compared to single RPB process and 28% to single PB. However, the operating cost depends on the price of electricity which can change with time.

Table 4. Impact of fluctuation in cost of electric power on total cost per year

Nominal Fluctuation in Electric Charge	RPB (Rotating packed bed)	PB (Packed bed)	RPB-PB (Superstructure)			
			Gross cost /year	Gas capacity distribution	Cost ratio of RPB and hybrid	Cost ratio of PB and hybrid
-80%	44.004	74.302	44.003	99.8% -RPB 0.2% - PB	0.999	0.592
-70%	46.710	75.88	46.380	99.6% -RPB 0.4% - PB	0.99	0.611
-50%	52.121	79.036	52.017	98.3% -RPB 1.7% - PB	0.998	0.658
-30%	57.531	82.194	56.624	69.5% -RPB 30.5% - PB	0.984	0.689
-20%	60.235	83.772	58.578	60.9% -RPB 39.1% - PB	0.973	0.699

-10%	62.940	85.35	60.417	54.6% -RPB 45.4% - PB	0.960	0.708
+10%	68.348	88.506	63.894	46.4%-RPB 53.6%- PB	0.935	0.722
+20%	71.052	90.071	65.569	43.4%-RPB 56.6%- PB	0.923	0.728
+30%	73.756	91.663	67.217	41.0%-RPB 59.0%- PB	0.911	0.733
+100%	92.681	102.711	78.354	32.1%-RPB 67.9%- PB	0.845	0.763
+200%	119.710	118.492	93.802	27.5%-RPB 72.5%- PB	0.784	0.792
+300%	146.734	134.274	109.061	25.6%-RPB 74.4%- PB	0.743	0.812
+400%	173.754	150.057	124.227	24.8%-RPB 75.2%- PB	0.715	0.828
+600%	227.786	181.62	154.386	24.1%-RPB 75.9%- PB	0.678	0.850
+900%	308.820	228.969	199.346	23.9%-RPB 76.1% - PB	0.646	0.871
+1200%	389. 844	276.317	244.082	24.1%-RPB 75.9% - PB	0.626	0.883
+2000%	605.855	402.576	362.682	24.4%-RPB 75.6% - PB	0.599	0.901

Table 4 shows for the parallel configuration (hybrid of RPB and PB in Fig. 3(b)) how the change in the price of electricity impacts the designs and the economics. The gap between the hybrid process and single RPB process shrinks as the electric price decreases and the optimization of the superstructure tends to choose the single RPB

process when the electricity price falls about 80% from the current price. On the other hand, the optimal design selects the hybrid process when the electric price increases. What is interesting is the hybrid process is still the best choice even when the electric price increases significantly.

6. Conclusion

The paper has developed nonlinear programming models for rotating packed bed (RPB), a novel apparatus involving process intensification, as well as for the conventional packed bed (PB). These models can predict flow and mass transfer performance of RPB and PB for given selection of design parameters (e.g. height, volume, rotating speed). Then a superstructure including both RPB and PB units was developed, and that considers configurations in series, in parallel and in between. The optimization of the superstructure was formulated as a nonlinear programming problem and the corresponding models were implemented in the modeling system GAMS. The application of the proposed synthesis model was demonstrated with a case study with H_2S removal from plant tail gas. The results were interesting in that they showed that the optimal configuration was a combination of both RPB and PB units in parallel. In order to study the effect of electric power cost, an analysis was performed that showed that greater proportion of the RPB was used as the cost of electric power decreases and the RPB still played an important role even the cost of electric power increase sharply.

NOMENCLATURE

D diffusivity, m^2/s

d_e the equivalent diameter of packing pore, m

G volumetric flow rate of gas, m^3/s

h height of packing, m

k_L liquid-phase mass transfer coefficient, m/s

L liquid flux, m/s

Q volumetric flow rate of the liquid, m^3/s

r radial position, m

r_b the length of end-effect zone, m

r_o the outer radius of the packing, m

r_i the inner radius of the packing, m

t time, s

u_θ the velocity of the θ direction, m/s

u_0 the initial velocity of jet flow, m/s

u_r the velocity of the r position, m/s

v_L kinematics liquid viscosity, m^2/s

Z axial width of packing, m

R geometric mean radius

R_{out} outer radius of rotator in RPB, m

R_{in} inner radius of rotator in RPB, m

$\bar{t}$ mean lifetime of the liquid film, s

y mole fraction of dissolvable i in gas

y_{in} mole fraction of dissolvable i inlet gas

y_{out} mole fraction of dissolvable i outlet gas

Greek Symbols

α specific area, m^2/m^3

ω rotating speed, rps

Abbreviations

CNY China Yuan

ACKNOWLEDGMENTS

This work was supported by the China Scholarship Council, the Center for Advanced Process Decision-making at Carnegie Mellon University and the Youth Plan Fund of University of Chinese Academy of Sciences (No. Y15101JY00). These institutions and programs are gratefully acknowledged.

REFERENCES

[1] Ramshaw C. The Incentive for Process Intensification. *Proceedings of 1st International Conference of Process Intensification for Chemical Industry* 1995; London, 18:1.

[2] Stankiewicz AL, Moulijn JA. Process intensification: transforming chemical engineering. *Chem. Eng. Prog*. 2000; 22-34.

[3] Lutze P, Gani R, Woodley JM. Process intensification: a perspective on process synthesis. *Chem. Eng. Pro. Process intensification* 2010; 49(6): 3-11.

[4] Stankiewicz A. Reactive separations for process intensification: an industrial perspective. *Chemical Engineering and Processing* 2003; 42: 137-144.

[5] Weserberg AW, Stephanopoulos G. Studies in process synthesis - i. branch and bound strategy with list techniques for the synthesis of separation schemes. *Chem. Eng. Sci.* 1975; 30(8): 963-972.

[6] Moulijin JA, Stankiewicz A, Grievink J, Gorak A. Process intensification and process systems engineering: a friendly symbiosis. *Comput. Chem. Eng.* 2008; 32(1-2): 3-11.

[7] Ramshaw C, Mallinson RH. Mass Transfer Process. U.S. Patent 1981;4283255.

[8] Bucklin BW, Won KW. Higee contactors for selective H_2S removal and superdehydration. Laurance Reid Gas Conditioning Conference, University of Oklahoma, March 1987 .

[9] Kelleher T, Fair JR. Distillation studies in a high-gravity contactor. *Ind. Eng. Chem. Res.* 1996; 35(12): 4646-4655.

[10] Munjal S, Dudukovic MP, Ramachandran PA. Mass transfer in rotating packed beds. II. Development of gas−liquid and liquid− solid mass transfer coefficients. *Chem. Eng. Sci.* 1989; 44 (10): 2245−2256.

[11] Chen JF. High Gravity Technology and Application Chemical Industry Press of China, 2002.

[12] Lin CC, Liu WT. Ozone oxidation in a rotating packed bed. *J. Chem. Technol. Biotechnol.* 2003; 78(2-3): 138-141.

[13] Gardner NC. Polymer devolazation by rotating packed bed. The first

international workshop high gravity engineering and technology, Beijing, China, June 1996.

[14] Chen J, Wang Y, Zheng C, Jia Z. Synthesis of nano particles of $CaCO_3$ in a novel reactor. The second international conference on process intensification in practice, Antwerp, Belgium, October 21-23, 1997.

[15] Qian Z, Li ZH, Guo K. Industrial Applied and Modeling Research on Selective H_2S Removal Using a Rotating Packed Bed. *Ind. Eng. Chem. Res.* 2012; *51* (23): 8108–8116.

[16] Qian Z, Guo K. Modeling study on absorption of CO_2 by aqueous solutions of *N*-Methyldiethanolamine in rotating packed bed. *Ind. Eng. Chem. Res.* 2009; *48* (20):9261–9267.

[17] Guo K, Wen JW, Zhao Y, Wang Y, Zhang ZZ, Li ZX, Qian Z. Optimal Packing of a Rotating Packed Bed for H_2S Removal. *Environ. Sci. Technol.*, 2014; *48* (12): 6844–6849.

[18] Yan ZY, Ruan Q, Lin C. Hydrodynamics in a rotating packed bed. II. A mathematical model. *Ind. Eng. Chem. Res.* 2012; 51 (31): 10482−10491.